

Manganese superoxide dismutase

M Elizabeth Stroupe, Michael DiDonato and John A Tainer

Handbook of Metalloproteins

Edited by

Albrecht Messerschmidt, Robert Huber, Thomas Poulos and Karl Wieghardt

© John Wiley & Sons, Ltd, Chichester, 2001

Manganese superoxide dismutase

M Elizabeth Stroupe, Michael DiDonato and John A Tainer

The Scripps Research Institute, La Jolla, CA, USA

FUNCTIONAL CLASS

Enzyme; oxidoreductase; EC 1.15.1.1; dimer or tetramer that uses one manganese ion per subunit to catalyze the sequential reduction and oxidation of superoxide.

Manganese superoxide dismutase (MnSOD) directly affects superoxide ($O_2^{\cdot-}$) and hydrogen peroxide (H_2O_2) concentrations in prokaryotic cells and eukaryotic mitochondria. MnSOD acts through a two-step mechanism in which it reduces superoxide by one electron to form molecular oxygen and then oxidizes the superoxide radical as it donates two protons to make hydrogen peroxide.

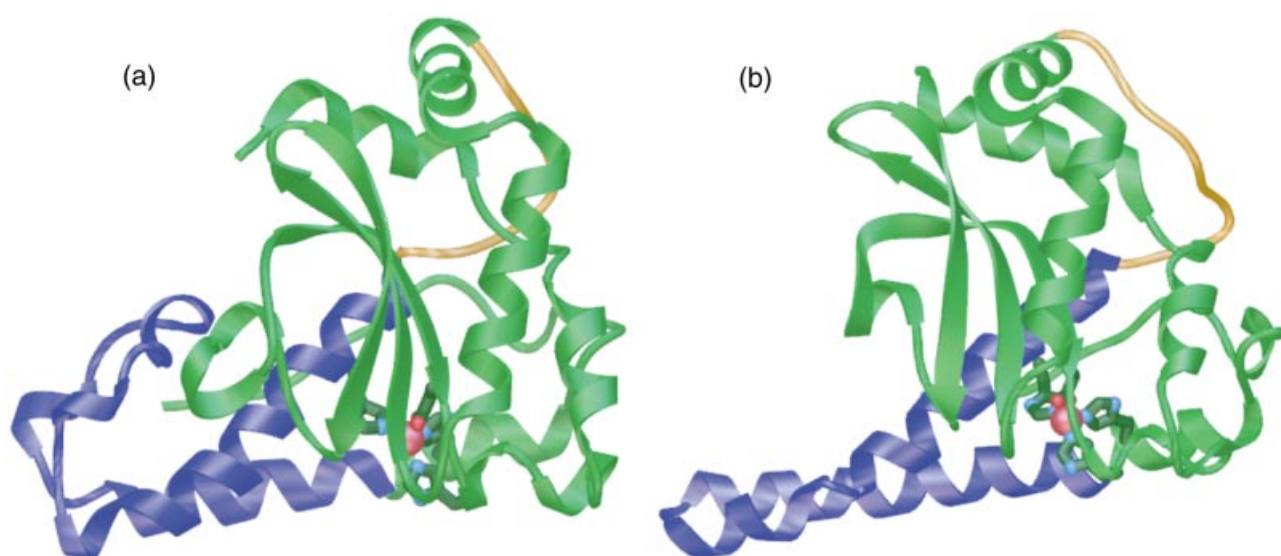
OCCURRENCE

Superoxide dismutase (SOD) is a ubiquitous enzyme that is found in all living organisms. At least three different folds, each of which uses either copper and zinc (Cu/ZnSOD), manganese or iron (Mn or FeSOD), or nickel (NiSOD),

perform the same reaction. The Fe- and MnSODs are structurally homologous enzymes with slightly different biological purpose. The *sodA* gene codes for MnSOD and its inducible expression is much more tightly regulated than that of FeSOD or Cu/ZnSOD.¹ The subunit fold and active-site metal placement of the *Escherichia coli* MnSOD (eMnSOD) and the human MnSOD (hMnSOD) exemplify variations of the prototypical fold for the Fe- or Mn-containing enzyme (3D Structure).

BIOLOGICAL FUNCTION

The primary function of MnSOD is to protect cells and mitochondria from free radical damage due to superoxide. Unlike the Cu/Zn- and Fe-containing enzymes, MnSOD expression in bacteria is induced under times of cellular stress^{1,2} as a result of exposure to a variety of elements including interleukin-1,³ tumor necrosis factor,⁴ paraquat,⁵ and X-ray radiation.⁶ The induction cascade is not fully understood; however, it is related to the superoxide



3D Structure of *E. coli* and human MnSOD (a) Ribbon diagram of the subunit from *E. coli* manganese superoxide dismutase. PDB code: 1VEW. (b) Ribbon diagram of the subunit from *H. sapiens* manganese superoxide dismutase. PDB code: 1ABM. In each schematic, the α -helical domain is blue and the α/β domain is green. The linker is yellow, the manganese is red, and the ligands to the metal are dark green. The figures were prepared with the Advanced Visualization Systems (AVS)⁷⁰ program.

response regulator (SoxR)-mediated pathway and correlates with both metal concentrations in the cell⁷ as well as the cell's redox environment, being activated when it is oxidative.⁸ In eukaryotes, MnSOD is targeted to the mitochondria after it is expressed in the nucleus.⁹ As over 90% of the dioxygen used by an organism is processed in the mitochondria,¹⁰ MnSOD primarily encounters reactive oxygen species formed as a result of mitochondrial function.

SOD enzymes are necessary for the integrity of an organism and the proper level of MnSOD expression in its specified cellular location is evidently critical for balancing both prokaryotic and eukaryotic cells' redox potential. SOD-deficient *E. coli* require rich media to grow aerobically, although they can grow on minimal media in an anaerobic environment.¹¹ That different SODs are found in different locations throughout the cell and are expressed with different frequencies suggests that they are suited to perform distinct roles in regulating reactive oxygen species.¹² For example, in *E. coli*, FeSOD accumulates in the periphery of the cell while MnSOD is found in the nucleoid, possibly binding non-specifically to DNA.¹³ Under some circumstances, MnSOD overexpression can also damage cells and when MnSOD-overexpressing *E. coli* are challenged with paraquat, their growth rate is slowed compared to cells that have only normal levels of MnSOD. In the cells that overexpress MnSOD there is a deficiency in glucose-6-phosphate dehydrogenase, an enzyme encoded by a gene within the SoxR regulon. This supports the hypothesis that the detrimental effect of too much MnSOD may reflect an incomplete response to cellular stress. An increase in H₂O₂ concentrations and the absence of superoxide, which would normally induce transcription of the SoxR regulon, leave the cell vulnerable to other instances of oxidative damage.¹⁴ MnSOD is found in the mitochondrial matrix of most eukaryotes¹⁵ and therefore mostly encounters superoxide produced during aerobic respiration. In contrast to the high mutation rate seen in mice lacking their cytosolic Cu/ZnSOD and subjected to traumatic injury, *sodA*-null mice do not live past three weeks, suggesting that MnSOD activity is necessary for sustained life in an aerobic environment.^{16,17}

Direct superoxide damage is not the only risk of aerobic life, for superoxide readily reacts with other small molecules to form additional, potentially damaging chemical species. For example, relative levels of superoxide and nitric oxide can be elevated during times of cellular stress, making the small molecules more likely to react and form the strongly oxidative molecule peroxynitrite (OONO⁻).¹⁸ Peroxynitrite, in turn, can react with nucleophilic amino acids, forming nitrated protein adducts with altered activity. When hMnSOD is treated with peroxynitrite, the peroxynitrite specifically nitrates Tyr34, thereby inactivating the enzyme.^{19,20} Nitrated hMnSOD has been implicated in some cases of organ transplant rejection; specifically,

MacMillan-Crow *et al.* suggest that nitrated, inactivate MnSOD may play a role in organ rejection.²¹ To balance superoxide and nitric oxide levels during normal cellular function, the NF- κ B pathway may help coordinate expression of hMnSOD and inducible nitric oxide synthase; however, the exact link is unknown.²²

AMINO ACID SEQUENCE INFORMATION

- *Homo sapiens* (human), precursor, 222 amino acid residues (AA), accession number (#): P04179.²³
- *Thermus thermophilus*, 204 AA, #: P09214.²⁴
- *Escherichia coli*, 206 AA, #: P00448, translated from genomic DNA.²⁵
- *Propionibacterium shermanii*, 201 AA, #: P80293, cambialistic.²⁶
- *Schizosaccharomyces pombe* (fission yeast), 218 AA, #: AAF19051 (direct submission, JH Jeong and JH Roe).
- *Saccharomyces cerevisiae* (budding yeast), 233 AA, #: P00447, translated from genomic DNA.²⁷
- *Arabidopsis thaliana* (thale cress), 213 AA, #: AAC24832, translated from cDNA.²⁸
- *Caenorhabditis elegans* (nematode), 218 AA, #: BAA12821, translated from cDNA.²⁹
- *Haemophilus influenzae* (influenza virus), 211 AA, #: CAA52054, translated from cDNA.³⁰

PROTEIN PRODUCTION, PURIFICATION, AND MOLECULAR CHARACTERIZATION

MnSOD overexpression and purification

Numerous overexpression and purification schemes are available for overproduction of a variety of species' MnSODs, including *E. coli*,^{25,31} *Thermus thermophilus*,³² and *Homo sapiens*.³³ The human enzyme was cloned from a library of human kidney cDNA and placed in the vector pCHMnSOD11aqlq. The protein was expressed in *E. coli* that lacked both SodA and SodB and supplemented with 2 mM MnCl₂. Purification after heat treatment to 60 °C over DE52 and CM52 columns resulted in fully active protein.³³

Oligomeric state

In prokaryotes, MnSOD is most commonly found as a dimer in which two monomers come together at a highly conserved interface.³⁴ The eukaryotic enzyme is usually tetrameric, formed when two of the prokaryotic-like dimers come together to form a dimer of dimers.^{33,35} Each subunit in the oligomer has one metal-binding active site, found at the junction of the two domains of which the monomer is composed (Figure 1).

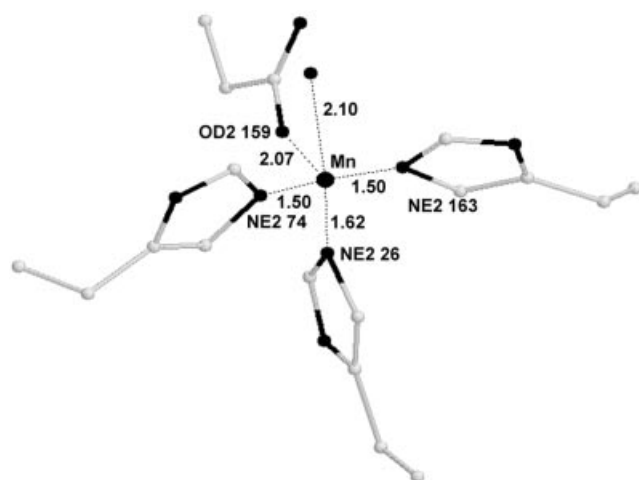


Figure 1 Ball and stick representation of the active site of MnSOD, showing bond lengths for the human enzyme. The figure was rendered in RASMOL.⁷¹

METAL CONTENT AND SPECIFICITY

Each monomer of MnSOD contains one manganese ion. The metal content of the enzyme is measured either by its characteristic absorbance at 480 nm or by using atomic absorbance spectroscopy.^{32,36,37} The protein scaffold binds either manganese or iron and differences in the bound metal do not preclude oligomerization.³⁸ Depending on the species, however, the enzyme is usually inactive when the non-physiological metal is bound.³⁹ Mutations far from the active site in the human enzyme affect the metal content, suggesting that metal selectivity is driven by residues not directly involved in metal ligation.⁴⁰ As the enzyme functions through a ping-pong mechanism,³⁷ it requires no cofactors to turn over substrate.

In addition to the commonly found Fe- or Mn-containing enzymes that only function with their endogenous metals, some SODs share the fold with this class and use Fe or Mn with equal efficiency to perform the oxidation and reduction of superoxide. Such SODs, called cambialistic SODs (cSODs), are found in some bacteria; the best characterized is from *Propionibacterium shermanii*;²⁶ however, cSODs have been found in *Streptococcus mutans*,⁴¹ *B. (Porphyromonas) gingivalis*,⁴² and *Aeropyrum pernix*.⁴³ The residues that directly chelate the metal are identical to those in Fe- or MnSOD and there is high homology in the second and third shell of residues that form the extended hydrogen bond network around the active site, thus the origin of metal selectivity is not obvious by sequence or structural alignment.

ACTIVITY TEST

SOD activity can be measured directly by following the disappearance of superoxide spectroscopically ($\lambda =$

250 nm, $\epsilon = 2000 \text{ M}^{-1} \text{ cm}^{-1}$). Superoxide can be generated either by dissolving KO_2 in aprotic solvent or by pulse radiolysis, in which an oxygen-saturated solution is exposed to a single electron pulse or an X-ray beam. By the KO_2 method, the enzyme and the substrate are mixed in a stopped flow apparatus and for the pulse radiolysis experiments, the enzyme is pre-equilibrated with the oxygen saturated solution.³⁷

SPECTROSCOPY

Although less commonly used in nature than either iron or copper, manganese is absolutely required for life.⁴⁴ Unlike iron and copper, manganese can access a wide range of oxidation states, from -3 to $+7$; however, like the other metals, the $+2$ and $+3$ oxidation states are the most biologically relevant. Relatively few manganese active sites have been characterized in detail; however, the mononuclear active site of MnSOD from several species^{45–47} has been extensively characterized by high-resolution X-ray crystallography and multiple forms of spectroscopy (UV/vis, CD, MCD, EPR). The following section will summarize the spectroscopic features of the MnSOD active site.

UV/vis spectroscopy

The absorption maximum of Mn(III)SOD occurs at approximately 478 nm with an extinction coefficient of $850 \text{ M}^{-1} \text{ cm}^{-1}$ per active site, imparting a pink color to the protein.³⁶ The broad, structured absorption spectrum for the Mn(III) active site spans the entire visible region and contains several characteristic features in addition to the 478 nm absorption maximum, including a partially resolved shoulder near 600 nm (the red band) and a notch near 485 nm.³⁶ The absorption in the visible region is composed of both broad and sharp features, shown by derivative absorption spectra that extend across the entire absorption envelope. Treatment with sodium dithionite reduces the Mn ion from the $+3$ to the $+2$ oxidation state, producing a colorless enzyme solution that retains SOD activity. As expected, the absorption spectrum of the Mn(II) enzyme lacks the characteristic features of the oxidized enzyme and therefore cannot be used to derive information about the reduced Mn center.

The major features of the Mn(III)SOD spectra result from the coordination geometry around the metal ion. The absorption maxima at 478 nm, which is characteristic of ligand field spectra from high spin Mn(III) ions, is higher in intensity than that typically measured for octahedral Mn(III) complexes,^{48,49} but it is consistent with intensities of five-coordinate Mn(III) complexes.³⁶ These spectroscopic results agree with X-ray crystallographic structures that show a five-coordinate active-site manganese with roughly trigonal bipyramidal (D_{3h}) or square pyramidal

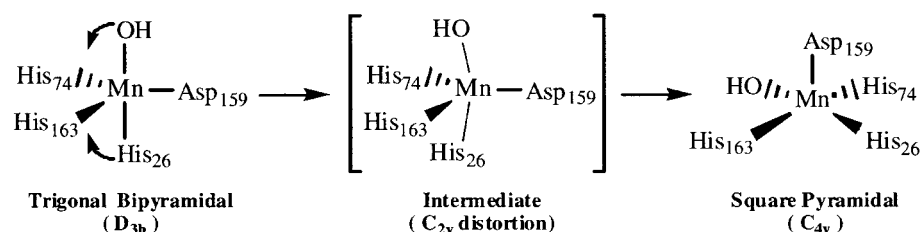


Figure 2 Schematic of the Berry pseudorotation, describing the active site for MnSOD.

(C_{4v}) geometry.^{50,51} Rotating an axial ligand of the D_{3h} species through a five coordinate intermediate structure with C_{2v} symmetry generates the C_{4v} species (Figure 2);³⁶ this operation is termed a Berry pseudorotation and is a useful construction for explaining the spectroscopic spectra from the Mn site. In the trigonal-bipyramidal arrangement, the d -orbitals are split into two doublets and a singlet in which the xz, yz -orbitals are the lowest in energy, followed by the x^2-y^2 , xy -orbitals and the z^2 -orbital. During Berry pseudorotation, the axial ligands move to equatorial positions in the square-pyramidal geometry, raising the x^2-y^2 orbital's energy with respect to the z^2 orbital. This transition also leads to significant mixing of the x^2-y^2 and z^2 orbitals in the intermediate C_{2v} structure.³⁶ The low energy transition at 600 nm is assigned to transitions between the mixed x^2-y^2 and z^2 orbitals and, based on model studies and classical ligand field theory, its energy is consistent with a manganese ion that has coordination number five.^{48,52-54}

CD and MCD spectroscopy

The CD spectra of MnSOD help characterize the ligand symmetry and geometry for the biologically important Mn(II) and Mn(III) oxidation states. The Mn(III)SOD enzyme exhibits several transitions between 350 and 800 nm.^{36,55} A negatively signed transition at 550 nm represents the strongest CD signal in this region and is well resolved from the lower energy red-band (600 nm), which appears as a positively signed shoulder.³⁶ Several poorly resolved features are seen between 375 and 460 nm. Reduction of the manganese ion to the +2 oxidation state leads to the loss of all CD spectral features in the 350–800 nm range. The MCD spectra of Mn(III)SOD exhibit two strong transitions, the first at 470 nm (positive) and the second at 593 nm (negative) that exhibit temperature-dependent MCD intensity.³⁶ The intensity of these transitions increases as the temperature decreases. The MCD spectra of the reduced enzyme is characterized by extremely weak low temperature transitions between 340 and 460 nm that are dominated by multiplets near 375, 390, and 430 nm.

The observed transitions in CD and the pattern of intensities in MCD suggest that the active site Mn(III) has lower-than-axial symmetry.³⁶ This interpretation is consistent with the hypothesized C_{2v} transition intermediate arising from a Berry pseudorotation between trigonal-bipyramidal and square-pyramidal geometries. In particular, the intense 550 nm transition in the CD spectra of Mn(III)SOD was assigned to d -orbital transitions between the z^2 and xz orbitals in C_{2v} symmetry, further supporting this intermediate's significance. Detailed spectroscopic studies employing various anionic ligands indicate that the Mn(III) site is closer to trigonal geometry in the native enzyme and shifts closer to square pyramidal geometry in the anion adducts.³⁶ The resulting changes in ground state orbital energies may have important implications for the redox chemistry of the site.

EPR spectroscopy

In the oxidized enzyme, Mn(III) has a high-spin d^4 electronic structure with four unpaired electrons ($S = 2$) and is EPR silent. The reduced Mn(II) active site has a high-spin d^5 electronic structure with five unpaired electrons ($S = 5/2$) and is EPR active. The helium X-band EPR spectra of reduced MnSOD has been measured by several groups and displays extremely complex resonances between 500 and 2250 G.^{36,51} Addition of various anionic ligands to the protein results in large perturbations of the EPR spectra that are anion specific. The zero-field splitting constant for the reduced enzyme is observed to be approximately one order of magnitude larger than for six-coordinate octahedral manganese complexes,⁵⁶ but is similar to that observed in distorted or lower coordination number species.⁵⁷ The large zero-field splitting constant is thought to arise from strong distortions of the axial positions in reduced MnSOD where the Mn(II) ions remains five-coordinate.⁵¹ Upon addition of exogenous ligands, the zero-field splitting constant decreases, consistent with a change in geometry around the Mn ion and correlating with changes observed in both CD and MCD spectra.

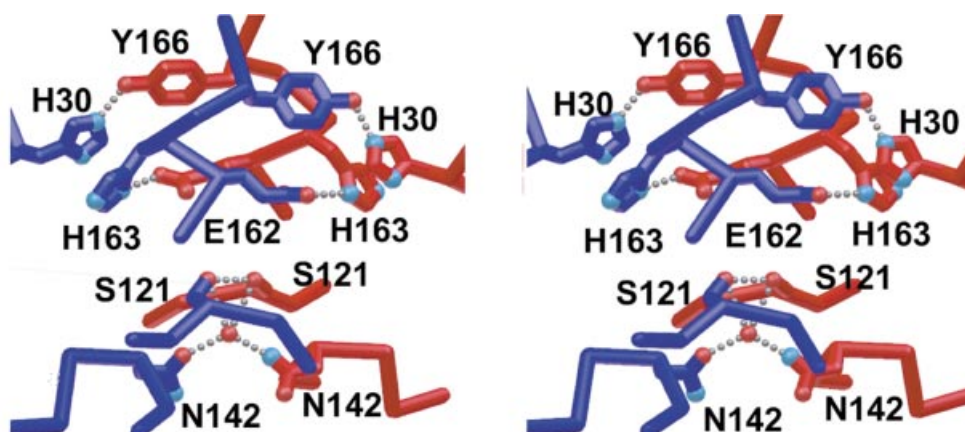


Figure 3 The symmetric dimer interface of hMnSOD, shown in stereo (rendered in AVS). Residues from each subunit are shown in either dark red or dark blue, oxygens are light red balls, nitrogens are blue balls, waters are red spheres, and hydrogen bonds are gray balls.

CRYSTALLOGRAPHY AND STRUCTURE

Crystallization

Crystal structures of MnSOD from four different species have been solved.^{33,58–60} Hexagonal crystals of the human MnSOD (hMnSOD) grow from ammonium sulfate or phosphate (2.0–2.7 M), buffered by either phosphate, citrate, or imidazole/malate at pH 7.5–8.5.³³ Other crystal forms grow from polyethylene glycol (PEG, MW 400, 600, 4000, or 10 000). High resolution data was obtained from orthorhombic crystals of hMnSOD grown from 24 to 30% PEG 400 at pH 7.5.³³

Description of the structure

MnSOD is a two-domain protein whose active site sits at the junction of the α -helical domain and the α/β domain,

shown in the 3D Structure. In all known MnSODs, three histidine residues, one monodentate aspartate, and a solvent molecule serve as ligands to the metal. The two-domain structure and the metal coordination are shared by FeSODs and cSODs with little difference in the specific interaction that define the active site. The human enzyme has the prototypical fold for this class and will be discussed in detail, followed by a comparison between the tetrameric human enzyme, the dimeric *E. coli* enzyme, and the tetrameric *T. thermophilus* enzyme.

Fold

The 22 kDa subunit of the human enzyme has 198 residues. The first 85 residues are a helical hairpin that is formed by two antiparallel helices connected by a hairpin turn and is the site of tetramerization. Two of the metal ligands, His26 and His74, come from the first and second

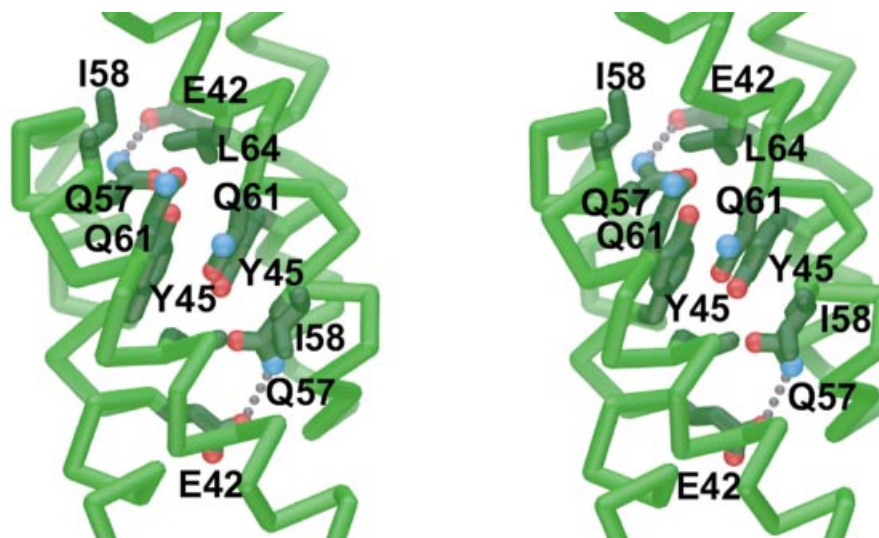


Figure 4 The hydrophobic residues along the helices that form the four helix bundle at the tetrameric interface of the human MnSOD, shown in stereo (rendered in AVS). The C_{α} trace of the backbone is light green, sidechains are dark green, oxygens are red balls, nitrogens are blue balls, and hydrogen bonds are gray balls.

helices of the helical hairpin, while Ile58 is found along the second helix near the hairpin turn. The last four residues in the second helix tighten into a 3_{10} -helix. The C-terminal 113 residues form the α/β domain, which begins with two short α -helices that are skewed relative to one another by about 105° . The residues that mediate dimerization are found in the C-terminal domain, and the two active sites are positioned within about 18 \AA of each other. A helix separates the second and third strands of the central, antiparallel, three-stranded β -sheet. The remaining ligands to the manganese, Asp159 and His163, come from the third β -strand and from the following coil. The C-terminal domain ends with two more helices skewed by about 100° to one another.³³

Dimer interface

A conserved set of interactions join the two-fold symmetric dimer in the human, *E. coli*, and *T. thermophilus* enzymes (Figure 3). Ser121 O_γ (*E. coli* Ser126, *T. thermophilus* Ser130) forms a hydrogen bond with its symmetry related partner from the second subunit, while the Asn142 side chain (145/150) forms water-mediated hydrogen bonds with the symmetric residue. Dimerization at this interface directly involves ligands to the metal through a hydrogen bond between His163 N_δ (171/170) on one subunit and Glu162's (170/169) carboxyl oxygen on the other subunit. A hydrogen bond network is hypothesized to pass protons to the Mn-bound solvent molecule and also extends across the dimer interface through a hydrogen bond between the N_ϵ of His30 (30/32) and the hydroxyl group of Tyr166 (174/173) from the other subunit.^{61–63}

Tetramer interface – human

The length and orientation of the α -helices from the N-terminal domain differs between the human and bacterial enzymes. In the human enzyme, the antiparallel helices extend two turns more than the helices in the bacterial enzymes, exposing an extensive hydrophobic surface on two pairs of helical hairpins from which the two four-helix bundles assemble to pull the dimers together. The side

chains along the exposed helical hairpins residues interdigitate as symmetry-related hydrophobic residues stack, resulting in a tight tetramer (Figure 4). The first helix and its two-fold symmetric partner interact as Glu42 and Tyr45 from each subunit stack along the length of the α -helix. A hydrogen bond between the Glu42 O_ϵ and the Gln57 N_ϵ in the symmetry-related subunit form an internal anchor between the first helix from one subunit and the second helix from the other. Gln57, Ile58, Gln61, and Leu64 stack with their symmetry-related partners from the adjacent subunit and pack against the second helices. The four helices associate to form a canonical four-helix bundle (Figure 5); the root mean square deviation of the main chain atoms is 2.25 \AA when the bundle from hMnSOD is superimposed on the four-helix bundle from tobacco mosaic virus coat protein (TMVcp, PDB code: 2TMV).³³ As a result of the tight interactions between subunits in the human enzyme, the distance between the Mn ions in two adjacent subunits in the tetramer is about 40.7 \AA and across the assembly the active sites are separated by about 42.0 \AA . While the human enzyme is exceptionally stable as a tetramer, a polymorphism in which residue 58 is a threonine rather than an isoleucine results in a protein that is predominantly a dimer in solution, with a melting point about 15° lower than that of the tetramer. Found at the tip of the helical hairpin, the polymorphism decreases the enzyme's stability by interfering with the hydrophobic interface of the four-helix bundle (Figure 3).⁴⁰

Tetramer interface – *T. thermophilus*

The thermostable *T. thermophilus* enzyme MnSOD (tMnSOD) tetramer is more open than that of the human MnSOD and the distances between manganese ions as defined above are 45.4 and 48.9 \AA . While domain one is all α -helical, as in the human enzyme, neither the *T. thermophilus* nor *E. coli* enzymes bear the extended α -helices, thus precluding formation of the four-helix bundle. Instead, the helices fold back at residues 46 and 68 (tMnSOD numbers), like the *E. coli* protein, splitting the long α -helices into two shorter helices and creating a more

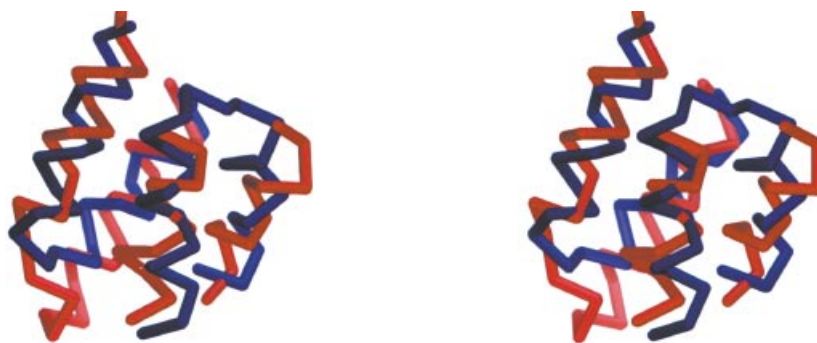


Figure 5 The overlay of the four-helix bundles from the tetrameric interface of hMnSOD (red) and the coat protein from tobacco mosaic virus (blue). The image is shown in stereo and was made with *AVS*.

compact monomer (3D Structure). When the human tetramer is superimposed on the *T. thermophilus* enzyme, however, the four-helix bundle from the human enzyme lies on top of the bent helices from the bacterial enzyme (Figure 6). *T. thermophilus* Val55, which sits at the tip of the folded hairpin that links the helices, packs back into the helices from the same subunit similar to the way in which the human Val54 packs against the helices from the symmetry related protein molecule. Lacking the extended hydrophobic surface, however, the *T. thermophilus* enzyme assembles by a series of direct and water-mediated hydrogen bonds across the interface that trap three structural water molecules. When monomers from the human and *T. thermophilus* enzymes are superimposed, the different tetrameric interfaces result in a more extended dimer in the *T. thermophilus* enzyme (Figure 7).

Metal geometry and metal specificity for catalysis

Four amino acid side chains and one solvent molecule coordinate the manganese ion in a strained trigonal bipyramidal geometry in both the reduced (Mn(II)) and oxidized (Mn(III)) states. Two of the amino acids that bind the Mn ion come from the all-helical domain, two come

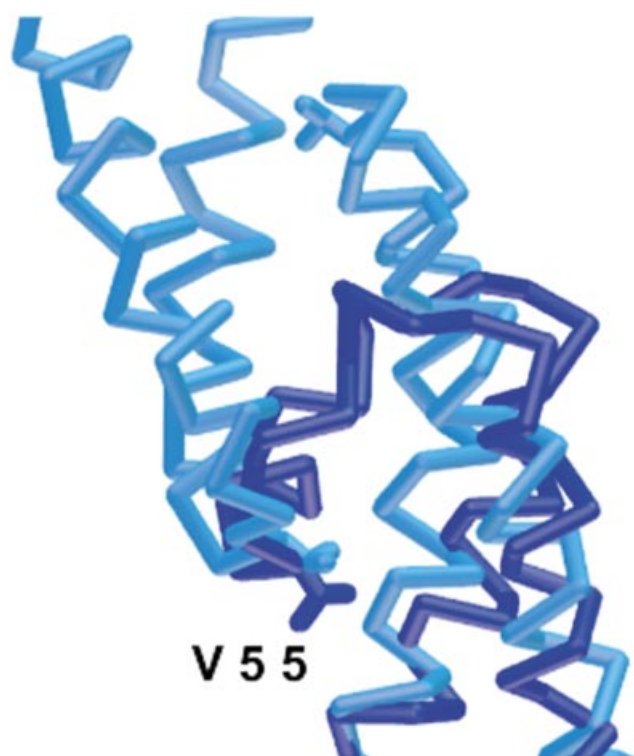


Figure 6 A superimposition of helical domains from the *T. thermophilus* (dark blue) and *H. sapiens* (light blue), showing the similar role of a valine at the tip of each helix. The figure was rendered in AVS.

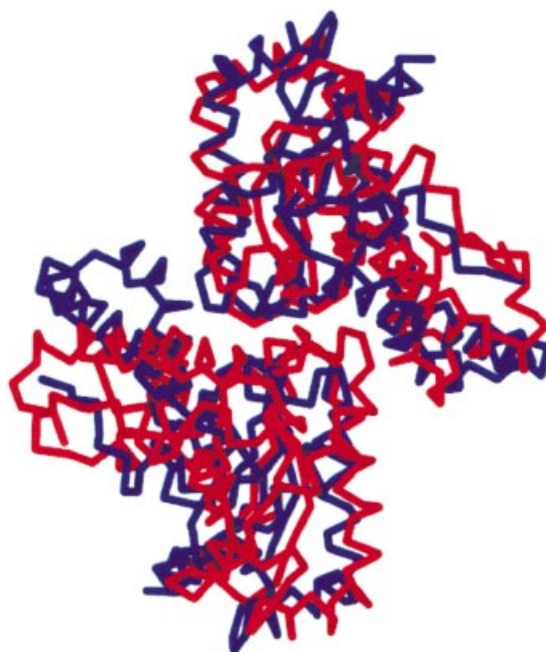


Figure 7 Superimposition of one subunit from *T. thermophilus* (red) and *H. sapiens* (blue) dimers, showing the more extended assembly from the thermophilic organism. The figure was rendered in AVS.

from the mixed α/β domain, and the active site is at the junction of these two domains. An extended hydrogen bond network connects the active site of one monomer with the two-fold symmetric subunit involved in making the active dimer.

Early in the study of the iron and manganese SODs, Yamakura noted that the enzymes were not active according to the standard activity assay when the endogenous metal was replaced by the other metal.^{39,64} Both polypeptides bind either metal with nearly equal affinity and the reconstituted enzymes bind substrate analogs, suggesting that the lack of activity is not due to a structural flaw in the reconstituted enzyme.^{65–67} A structure of the Fe-substituted eMnSOD (Fe-subMnSOD) enzymes revealed that the five-coordinate metal had expanded to include an extra molecule of solvent, likely a hydroxide ion.⁵⁸ Recently, Vance and Miller showed that Fe(II)-subMnSOD could reduce substrate, based on the observation that Fe(II)-subMnSOD was oxidized in the presence of superoxide; however, Fe(III)-subMnSOD was not reduced in the presence of substrate.⁶⁶ Taken together, these results suggest that the reduced metal-substituted enzyme can bind substrate and pass an electron to it, but that either substrate binding or electron transfer (or both) do not occur in the oxidized enzyme; the substituted enzyme can perform only half of its enzymatic cycle. Furthermore, the substituted, reduced enzyme can be fully oxidized by superoxide below pH 6.7 (the pK_a of the substituted enzyme), refuting the suggestion that enzyme inhibition by hydroxide binding to the metal is the only

Manganese superoxide dismutase

cause for inactivation. Instead, Vance and Miller suggest that Fe-subMnSOD is unable to turnover because the E_0 of the metal is depressed below the optimal value of 0.2–0.4 V, making an enzyme that is physically unable to donate an electron to the substrate. According to their measurements, FeSOD's E_0 is 0.223 V and the E_0 for Fe-subMnSOD is -0.243 V, about a half an electron volt lower. The measurements correlate with the differences in redox potential between iron and manganese, supporting the hypothesis that the protein scaffold tunes the metal ion so that its redox potential is poised at the proper level to efficiently react with superoxide. Because iron and manganese have inherently different redox potentials, the protein must tune their activity differently, thus when the incorrect metal is incorporated, its redox potential is not set to perform both disproportionation reactions. Vance and Miller offer a valuable explanation for the limited activity of the metal substituted proteins. The structural basis for the tuning and for the selective binding of the correct metal *in vivo* remains poorly understood; however, the protein environment clearly helps to control enzyme activity and define metal specificity.

Hydrogen bonding network and catalysis

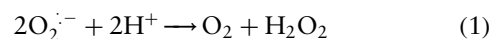
Structure-based mutagenesis of hydrogen bonding partners reveals residues outside the first shell of metal ligands that play an important role in controlling the enzyme's activity by forming an extended hydrogen bond network (Figure 8). In the wild-type structure of the human enzyme, the solvent molecule that coordinates the metal also forms a hydrogen bond with Gln143 N_ε, which subsequently

hydrogen bonds to the Tyr34 hydroxyl group. A conserved water molecule mediates a hydrogen bond between Tyr34 and His30, which also forms a hydrogen bond with Tyr166 from another subunit. Changes in any of these residues significantly affects both the enzyme's catalytic activity and stability,^{61–63} despite minimal structural changes in the active site. The network also extends from other ligands to the metal, encompassing a water-mediated hydrogen bond between Met23 and His26 and a hydrogen bond that forms across the dimer interface between His163 and Gln162.³³

FUNCTIONAL ASPECTS

Kinetics and catalytic properties of MnSOD

All SODs catalyze the degradation of the superoxide radical to molecular oxygen and hydrogen peroxide regardless of the catalytic metal used (Equation 1).



The overall reaction is a redox process that involves the alternate oxidation and reduction of the catalytic active site metal. In the first step, superoxide binds to the resting enzyme (Mn(III)), is oxidized to molecular oxygen, and reduces the manganese to the +2 oxidation state (Equation 2). In the second step, a second molecule of superoxide binds to the reduced enzyme (Mn(II)), is reduced to hydrogen peroxide, and oxidized the manganese back to the resting +3 state (Equation 3).

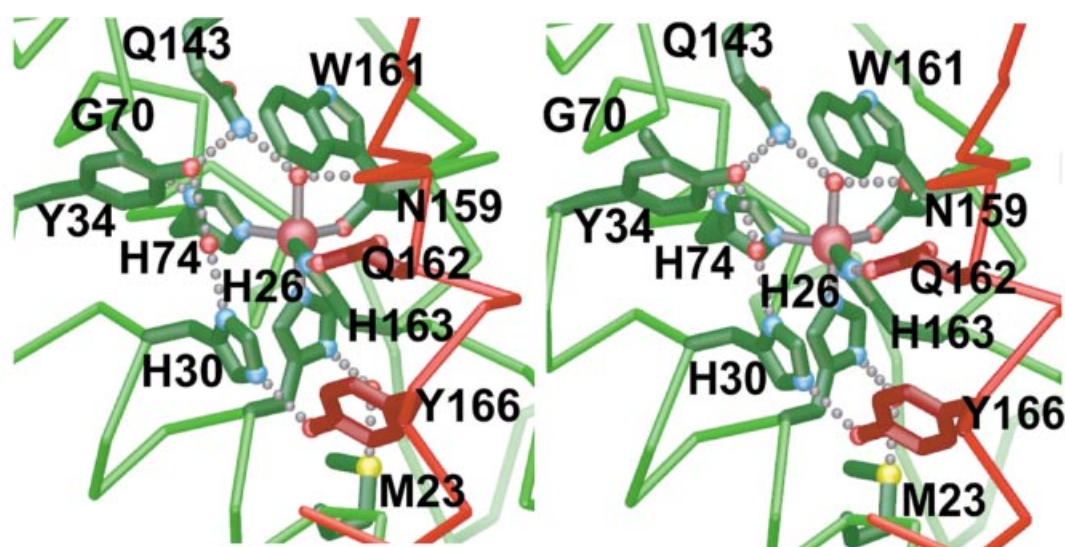
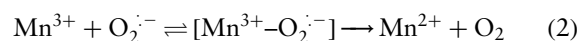


Figure 8 A stereo view of the hydrogen bonding network surrounding the manganese-containing active site (rendered in AVS). The C_α trace of the subunit whose active site is shown is light green while the C_α trace of its dimeric partner is light red. Side chains are dark green or dark red, respectively. The manganese is dark pink, oxygens are red balls, nitrogens are blue balls, sulfurs are yellow balls, waters are red spheres, and hydrogen bonds are gray balls.

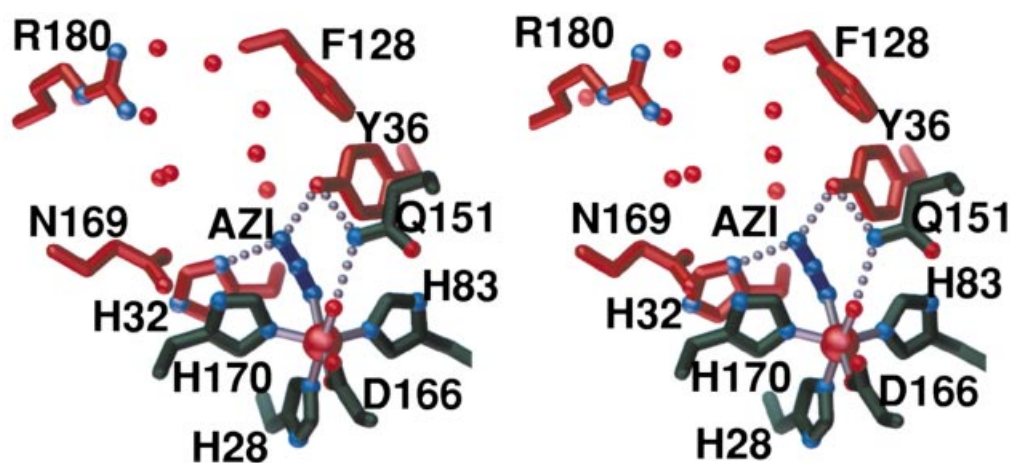
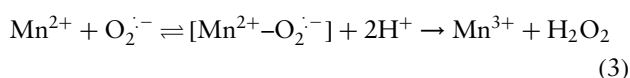


Figure 9 A stereo view of the azide-bound form of *T. thermophilus* MnSOD. The residues that coordinate the manganese and Gln151 are green, while the residues that line the channel leading to the azide are dark red. The azide is dark blue, oxygens are red balls, nitrogens are light blue, water molecules are red spheres, and hydrogen bonds are gray spheres. The figure was rendered in avs.



Detailed kinetic studies on hMnSOD using stopped-flow spectrophotometry and pulse radiolysis have shown that its kinetic constants are very similar to those measured for MnSOD from *T. thermophilus* ($k_{\text{cat}} = 4 \times 10^4 \text{ s}^{-1}$, $k_{\text{cat}}/K_{\text{m}} = 2 \times 10^9 \text{ M}^{-1} \text{ s}^{-1}$ for human MnSOD, $1.3 \times 10^4 \text{ s}^{-1}$ and $3 \times 10^8 \text{ M}^{-1} \text{ s}^{-1}$ respectively for tMnSOD).³⁷ A major difference between the two enzymes is the rate of formation of the inhibited state. The inactive state has been observed spectrophotometrically in the *T. thermophilus* enzyme and has been postulated to contain a side-on complex of Mn(III) and peroxide (Mn(III)O_2^{2-}).^{37,68} In the human enzyme the formation of this complex is 30 times faster than in the *T. thermophilus* enzyme.³⁷ The nature of this increase in rate is not yet completely understood.

Both the kinetic rate and absorption maxima of MnSOD show pH dependence. The molar absorptivity at 480 nm shows a sigmoidal response to varying pH, decreasing as pH increases.³⁷ This behavior could be integrated into the theory by considering an ionizable group with a pK_a of 9.4. The first order rate constant also shows pH dependence in the range of 8.4 to 10.0, decreasing at the higher pH values. Tyr34 was implicated as the ionizable group giving rise to this pH dependence since its side chain is only 5 Å away from the active site manganese in the human enzyme.³³ Mutation of Tyr34 to Phe abolishes the pH dependence of the absorption spectra and results in an enzyme which is more susceptible to product inhibition.³⁷ Together, these observations implicate Tyr34 as important in the catalytic cycle of the enzyme.

FUNCTIONAL DERIVATIVES

Azide-bound structure

As predicted by early spectroscopic studies,³⁶ structures of tMnSOD and eFeSOD in complex with azide show that azide coordinates directly to the metal ion in both the Fe- and Mn-containing enzymes without causing release of the metal-coordinated solvent molecule.⁶⁹ The increased coordination number of the metal opens the His-Mn-His angle to 148° and the bent azide molecule binds across from the aspartate ligand, forming hydrogen bonds with the His32 N_δ and with the Tyr36 hydroxyl (Figure 9). The molecule points towards the solvent-filled channel formed by His32, Tyr36, Phe128, Glu169, and Arg180. Direct coordination supports an inner shell mechanism for electron transfer to the substrate rather than outer shell coordination of the substrate. While the azide is bound in a slightly different orientation in the *E. coli* azide-bound FeSOD structure, it also increases the coordination number of the iron to six.⁶⁹

Mutants

In all of the known structures of MnSODs, an extensive network of hydrogen bonds extends from the Mn-bound solvent to the solvent accessible surface, providing a possible mechanism for delivering protons to the active site and a means by which the pK_a of the active-site water is regulated. The Gln143Asn, Gln143Ala, Tyr34Phe, Trp161Phe, His30Ala, His30Ser, His30Gln, His30Asn, His30Lys, His30Glu, and Tyr166Phe mutants^{61–63} made in the human enzyme, were characterized both biochemically and structurally to ascertain the role of each residue. Most substitutions at Gln143 create an enzyme whose activity is about 2 to 3 orders of magnitude lower than in

the wild-type. The structures of both the Gln143Asn and Gln143Ala enzymes were solved and, in both instances, a water molecule has replaced the endogenous side chain, fulfilling the necessary interactions to compliment the hydrogen bond network.^{61,72} The low activity of the enzymes suggests that maintenance of the hydrogen bond network at this site is sufficient for turnover, but the chemical properties of the hydrogen bond partners tunes the reactivity of the active site. The Tyr34Phe mutant has a steady-state turnover resembling that of the wild-type enzyme, but at high superoxide levels the rate decreases by 10-fold. The structure shows that the phenylalanine ring sits in about the same orientation as the tyrosine ring and no water molecule intercedes to compliment the broken hydrogen bond network. The lower rate at high superoxide concentration suggests that proton transfer is only hindered in the presence of saturating concentrations of superoxide.⁶² In the wild-type structure, Trp161 sits at the edge of the active site cavity, stacking against the Mn-bound solvent molecule. When it is replaced by phenylalanine, the enzyme remains almost fully active. The hydroxyl of Tyr34 is about 1.2 Å closer to the manganese than in the wild-type structure, leading to a more compact network of hydrogen bonds about the active site. Changing His30 to each of the above mentioned residues lowered the k_{cat}/K_m by about one order of magnitude, suggesting that there is some flexibility in the chemical properties of residue 30 but that a histidine in this position creates the most efficient enzyme; the His30Glu mutant is the least active, perhaps because of substrate repulsion by the negative charge.⁶³ Like most of the His30 mutants, Tyr166Phe showed a decrease in k_{cat}/K_m of about an order of magnitude.⁶³

CONCLUSIONS

MnSOD contains one of the few manganese sites whose activity and structure has been sufficiently well characterized to establish an elegant link between chemistry, biology, and medicine. Chemically, MnSODs exhibit remarkable metal specificity in view of the structural similarities between the iron- and manganese-containing enzymes. Having such similar tertiary structures, the Fe- and MnSODs offer a unique system in which to study the subtle effects that a protein neighborhood has on metal ion activities including tuning their redox potentials for efficient catalysis. Biologically, the differences between expression and activity patterns of the three commonly found SODs (Fe, Mn, and Cu/Zn) demonstrate how organisms control and balance reactive oxygen species in the cellular environment. This detailed knowledge about the structure and the enzyme kinetics of the human MnSOD enzyme should help to explain the properties of polymorphisms found in the gene, including their implications for human health.

REFERENCES

- 1 HM Hassan and LW Schrum, *Microbiol Rev*, **14**, 315–23 (1994).
- 2 HM Hassan and I Fridovich, *Eur J Rheumatol Inflamm*, **4**, 160–72 (1981).
- 3 GA Visner, WC Dougall, JM Wilson, IA Burr and HS Nick, *J Biol Chem*, **265**, 2856–64 (1990).
- 4 A Masuda, DL Longo, Y Kobayashi, E Appella, JJ Oppenheim and K Matsushima, *FASEB J*, **2**, 3087–91 (1988).
- 5 J Krall, AC Bagley, GT Mullenbach, RA Hallewell and RE Lynch, *J Biol Chem*, **263**, 1910–14 (1988).
- 6 LW Oberley, DK St Clair, AP Autor and TD Oberley, *Arch Biochem Biophys*, **254**, 69–80 (1987).
- 7 CT Privalle and I Fridovich, *J Biol Chem*, **267**, 9140–5 (1992).
- 8 BB Warner, L Stuart, S Gebb and JR Wispe, *Am J Physiol*, **271**, L150–8 (1996).
- 9 YS Ho and JD Crapo, *FEBS Lett*, **229**, 56–260 (1988).
- 10 B Chance, H Sies and A Boveris, *Physiol Rev*, **59**, 527–605 (1979).
- 11 A Carlioz and D Touati, *EMBO J*, **5**, 623–30 (1986).
- 12 KA Hopkin, MA Papazian and HM,

- 30 JS Kroll, PR Langford, JR Saah and BM Loynds, *Mol Medicine*, **10**, 839–48 (1993).
- 31 D Touati, *J Bacteriol*, **155**, 1078–87 (1983).
- 32 S Sato and K Nakazawa, *J Biochem (Tokyo)*, **83**, 1165–71 (1978).
- 33 GE Borgstahl, HE Parge, MJ Hickey, WF Beyer Jr, RA Hallewell and JA Tainer, *Cell*, **71**, 107–18 (1992).
- 34 RA Edwards, HM Baker, MM Whittaker, JW Whittaker, GB Jameson and EN Baker, *J Biol Inorg Chem*, **3**, 161–71 (1998).
- 35 UG Wagner, KA Patridge, ML Ludwig, WC Stallings, MM Werber, C Oefner, F Frolow and JL Sussman, *Protein Sci*, **2**, 814–25 (1993).
- 36 JW Whittaker and MM Whittaker, *J Am Chem Soc*, **113**, 5528–40 (1991).
- 37 JL Hsu, Y Hsieh, C Tu, D O'Connor, HS Nick and DN Silverman, *J Biol Chem*, **271**, 17687–91 (1996).
- 38 A-F Miller and DL Sorkin, *Comments Mol Cell Biophysics*, **9**, 1–48 (1997).
- 39 F Yamakura, *J Biochem (Tokyo)*, **83**, 849–57 (1978).
- 40 GE Borgstahl, HE Parge, MJ Hickey, MJ Johnson, M Boissinot, RA Hallewell, JR Lepock, DE Cabelli and JA Tainer, *Biochemistry*, **35**, 4287–97 (1996).
- 41 ME Martin, BR Byers, MO Olson, ML Salin, JE Arceneaux and C Tolbert, *J Biol Chem*, **261**, 9361–7 (1986).
- 42 SM Jackson and JB Cooper, *Biometals*, **11**, 159–73 (1998).
- 43 S Yamano, Y Sako, N Nomura and T Maruyama, *J Biochem (Tokyo)*, **126**, 218–25 (1999).
- 44 CL Keen, B Lonnerdal and LS Hurley, *Biochemistry of the Essential Ultratrace Elements*, Plenum, New York (1984).
- 45 BBJ Keele, JM McCord and I Fridovich, *J Biol Chem*, **245**, 6176–81 (1970).
- 46 J Lumsden, R Cammack and DO Hall, *Biochim Biophys Acta*, **438**, 389–92 (1976).
- 47 JM McCord, JA Boyle, EDJ Day, LJ Rizzolo and ML Salin, *Superoxide and Superoxide Dismutases*, Academic, New York (1977).
- 48 TS Davis, JP Fackler and MJ Weeks, *Inorg Chem*, **8**, 1994–2002 (1968).
- 49 ABP Lever, *Inorganic Electronic Spectroscopy*, Elsevier, New York (1984).
- 50 WC Stallings, KA Patridge, RK Strong and ML Ludwig, *J Biol Chem*, **259**, 10695–9 (1984).
- 51 WC Stallings, KA Patridge and ML Ludwig, *Superoxide and Superoxide Dismutase in Chemistry, Biology and Medicine*, Elsevier, New York (1986).
- 52 R Dingle, *J Mol Spectrosc*, **9**, 426–7 (1962).
- 53 R Dingle, *Inorg Chem*, **4**, 1287–90 (1965).
- 54 R Dingle, *Acta Chem Scand*, **20**, 33–44 (1966).
- 55 BBJ Keele, C Giovagnoli and G Rotillio, *Physiol Chem Physics*, **7**, 1–6 (1975).
- 56 HA Kuska and MT Rogers, *Radical Ions*, Interscience, New York (1968).
- 57 RB Birdy, G Brun, DML Goodgame and M Goodgame, *J Chem Soc Dalton Trans*, 149–51 (1979).
- 58 RA Edwards, MM Whittaker, JW Whittaker, GB Jameson and EN Baker, *J Am Chem Soc*, **120**, 9684–5 (1998).
- 59 ML Ludwig, AL Metzger, KA Patridge and WC Stallings, *J Mol Biol*, **219**, 335–58 (1991).
- 60 MW Parker and CC Blake, *J Mol Biol*, **199**, 649–61 (1988).
- 61 Y Hsieh, Y Guan, C Tu, PJ Bratt, A Angerhofer, JR Lepock, MJ Hickey, JA Tainer, HS Nick and DN Silverman, *Biochemistry*, **37**, 4731–9 (1998).
- 62 Y Guan, MJ Hickey, GE Borgstahl, RA Hallewell, JR Lepock, D O'Connor, Y Hsieh, HS Nick, DN Silverman and JA Tainer, *Biochemistry*, **37**, 4722–30 (1998).
- 63 CA Ramilo, V Leveque, Y Guan, JR Lepock, JA Tainer, HS Nick and DN Silverman, *J Biol Chem*, **274**, 27711–6 (1999).
- 64 DE Ose and I Fridovich, *Arch Biochem Biophys*, **194**, 360–4 (1979).
- 65 F Yamakura, K Kobayashi, H Ue and M Konno, *Eur J Biochem*, **227**, 700–6 (1995).
- 66 CK Vance and A-F Miller, *J Am Chem Soc*, **120**, 461–7 (1998).
- 67 CK Vance and AF Miller, *Biochemistry*, **37**, 5518–27 (1998).
- 68 C Bull, EC Niederhoffer, T Yoshida and JA Fee, *J Am Chem Soc*, **113**, 4076–96 (1991).
- 69 MS Lah, MM Dixon, KA Patridge, WC Stallings, JA Fee and ML Ludwig, *Biochemistry*, **34**, 1646–60 (1995).
- 70 C Upson, T Faulhabe, D Kamins, D Laidlaw, D Schlegel, J Vroom, R Gurwitz and A Vandam, *IEEE Comp G*, **9**, 30–42 (1989).
- 71 R Sayle and EJ Milner-White, *TIBS*, **20**, 333–79 (1995).
- 72 VJ-P Leveque, ME Stroupe, JR Lepock, DE Cabelli, JA Tainer, HS Nick and DN Silverman, *Biochemistry*, **39**, 7131–7 (2000).